

Physical Properties of Parabens and Their Mixtures: Solubility in Water, Thermal Behavior, and Crystal Structures

FERDINANDO GIORDANO,^{*,†} RUGGERO BETTINI,[†] CRISTINA DONINI,[†] ANDREA GAZZANIGA,[‡] MINO R. CAIRA,[§] GEOFFREY G. Z. ZHANG,^{||,⊥} AND DAVID J. W. GRANT^{||}

Contribution from *Dipartimento Farmaceutico, University of Parma, Viale delle Scienze, 43100 Parma, Italy, Istituto Chimico Farmaceutico, University of Milan, Viale Abruzzi 43, 20131 Milan, Italy, Department of Chemistry, University of Cape Town, Rondebosch 7701, South Africa, and Department of Pharmaceutics, College of Pharmacy, University of Minnesota, Weaver-Densford Hall, 308 Harvard Street, S. E., Minneapolis, Minnesota 55455-0343.*

Received February 9, 1999. Final revised manuscript received June 28, 1999.
Accepted for publication August 30, 1999.

Abstract □ The peculiar solubility behavior of propylparaben (propyl ester of 4-hydroxybenzoic acid) in aqueous solution, when tested separately and together with methyl-, ethyl-, and butyl-parabens, has been investigated in detail. The results clearly indicate that the decrease in solubility ($\approx 50\%$ compared to the solubility value of propylparaben alone) is typical of those mixtures containing also ethylparaben, as demonstrated by solubility experiments on binary, ternary, and quaternary mixtures of the parabens. Phase diagrams of all the six binaries show that propylparaben and ethylparaben are the only pair that form almost ideal solid solutions near the melting temperatures. Moreover, phase-solubility analysis shows that propylparaben and ethylparaben, at room temperature, can also form solid solutions whose solubility is related to the composition of the solid phase at equilibrium. To achieve an independent confirmation of the possible solid solution formation that supports the above interpretation of the solubility behavior, the crystal structures of the four parabens have been examined and isostructurality has been found to exist only between ethylparaben and propylparaben. Powder X-ray diffraction has also been performed on ethylparaben, propylparaben, and their solid solutions obtained by recrystallization from water. The progressive shift of distinctive diffraction peaks with phase composition clearly indicates that propylparaben and ethylparaben form substitutional solid solutions. The small value (<1) of the disruption index provides thermodynamic support for substitutional solid solutions based on isostructural crystals.

Introduction

Parabens (esters of 4-hydroxybenzoic acid) are preservatives widely used in cosmetics, food products, and pharmaceutical formulations. Parabens are generally used in combination to take advantage of synergistic effects, are active over a wide pH range, have a broad spectrum of antimicrobial activity, and are most effective against yeasts and molds.¹ The antimicrobial activity of the parabens increases as the chain length of the alkyl moiety is increased; their aqueous solubility, however, decreases, so the sodium salts of the parabens are also frequently used in formulations. An alternative approach to increasing

solubility is the use of cyclodextrin complexation. Many reports²⁻⁴ deal with the formation of inclusion compounds with natural and semisynthetic cyclodextrins to increase the aqueous solubility of selected parabens.

Recently⁵ the solubilities of four parabens (methyl, ethyl, propyl, and butyl esters) have been measured singly and together in water and in aqueous solutions of 2-hydroxypropyl- β -cyclodextrin. Aqueous solubilities (without 2-hydroxypropyl- β -cyclodextrin) of all parabens were found to agree well with literature values^{6,7} when determined separately. Rather surprisingly, however, when the solubilities in water at 25 °C of the four parabens were measured together, the solubility of propylparaben was found to be reduced by approximately 50%, with relatively small increases or decreases (within 10%) for methyl-, ethyl-, and butyl-paraben.

Changes of solubility generally can be attributed to the formation of hydrates, recrystallization of more stable polymorphs, or interaction phenomena in solution as well as in the solid state.⁸⁻¹¹ In the system under investigation, it is intriguing and stimulating that the solubility of only one component (propylparaben) seemed to be significantly affected when tested in the combination of four homologues. The massive decline of propylparaben solubility has hitherto remained unexplained: furthermore no evaluation of the physical nature or chemical composition of the solid phases present at equilibrium has been reported.

Aiming to find a plausible explanation for the unpredictable behavior described above for propylparaben⁵ we report here the results of investigations with the same four homologues (methyl- (M), ethyl- (E), propyl- (P), and butyl- (B) paraben). In particular, the solubilities in water of each paraben from the binary, ternary, and quaternary mixtures are measured. The solid phases recovered at equilibrium from solubility experiments are characterized by their thermal behavior, using differential scanning calorimetry (DSC), thermogravimetry (TGA), and hot stage microscopy (HSM), by their composition using high performance liquid chromatography (HPLC), and by their structural properties, using powder X-ray diffractometry (PXRD). The solubility profiles at ambient temperature are also investigated by means of phase solubility analysis as suggested by Higuchi and Connors.¹² Moreover, the phase diagrams of all possible binaries are drawn from DSC measurements and compared with the corresponding calculated ones.

Finally, to complete the physicochemical characterization and to accomplish a comprehensive understanding of the solid state properties of these compounds by relating molecular scale properties and bulk properties, the crystal structures of propylparaben and butylparaben are also determined and critically evaluated together with those of

* Corresponding author: Tel: +39-0521-905079, fax: +39-0521-905006, e-mail: giordano@unipr.it.

[†] University of Parma.

[‡] University of Milan.

[§] University of Cape Town.

^{||} University of Minnesota.

[⊥] Present address: Abbott Laboratories, Department 04P3, Building AP9, 100 Abbott Park Road, Abbott Park, IL 60064-6120.

methyl paraben and ethyl paraben whose crystallographic data have been reported previously.^{13,14}

Experimental Section

Materials—Methyl-, ethyl-, propyl-, and butyl-paraben were obtained from Sigma Chemical Company (St. Louis, MO) and were used as received. Organic solvents were of chromatographic grade purity. Double-distilled water was used for solubility experiments and buffer preparation.

Aqueous Solubility—The solubility in water for each paraben, singly or from the binary, ternary, and quaternary mixtures, was determined by equilibrating the liquid phase with a known weight of each component in powdered form at 25.0 ± 0.5 °C with agitation. In all cases, a 5-day period had previously been shown to afford equilibrium. Three independent sets of experiments were performed on single components or their combinations.

Recrystallization from Water—Mixtures containing E and P in molar ratios of 1:1 and 1:2 were recrystallized from water by dissolving 200 mg of the mixture in 200 mL of water at 75 °C and allowing, after filtration, the spontaneous cooling to ambient temperature. The crystalline solid phase which separated at equilibrium was recovered by vacuum filtration: both the filtrate and the solid phase were analyzed for E and P contents by HPLC.

HPLC Analysis—Samples of the solution under examination, appropriately diluted with the mobile phase (methanol/0.04 M ammonium acetate, 55:45, v:v), were analyzed with an HPLC system (LC-10 AS Shimadzu, Japan); detector (UV-vis, SPD-10A Shimadzu) at $\lambda = 256$ nm; column (C-18 BondapaK, Waters, Milford, MA) 10 μ m, 3.9×300 mm; flow rate 0.8 mL min⁻¹. Peak integration was performed with a C-R6A Cromatopac (Shimadzu, Japan). Linearity of response in the 0–20 mg mL⁻¹ concentration range was assessed for each compound from plots of peak area against concentration.

Thermal Analyses—Differential scanning calorimetry (DSC) and thermogravimetry (TGA) were performed by means of a Mettler 821e STAre system and a TG50 cell (Mettler Toledo, Switzerland): hot stage microscopy (HSM) was carried out with a HFS 91 Linkam hot stage (Linkam, UK) and a Nikon Labophot microscope (Nikon, Japan).

Experimental phase diagrams of binary systems were constructed by plotting melting temperatures taken from DSC curves versus composition. Solid mixtures of each binary system were prepared by combining appropriate volumes of methanolic solutions with known concentrations of each paraben and slowly evaporating the solvent under reduced pressure. Four to six samples for each mixture were scanned at 10 K min⁻¹ from 40 °C to a temperature 10 K above the melting point of the higher melting component under a flux of dry nitrogen (100 mL min⁻¹).

Calculation of the liquidus curves was performed using the Schröder–Van Laar equation¹⁵ in its simplified form:

$$\ln x = \frac{\Delta H_A^f}{R} \left(\frac{1}{T_A^f} - \frac{1}{T^f} \right)$$

where x is the mole fraction of the more abundant component of a mixture whose melting terminates at T^f (in Kelvin), ΔH_A^f (cal mol⁻¹), and T_A^f (also in Kelvin) are the enthalpy of fusion and the melting point of the pure component, respectively, and R is the gas constant, 1.9869 cal mol⁻¹ K⁻¹.

Phase Solubility Analyses on Binary Systems—Fixed amounts (approximately twice the quantity necessary for a saturated solution) of the accurately weighed paraben with increasing amounts (up to an excess with respect to its solubility) of the second paraben under investigation were placed in 100 mL flasks, which were then filled to volume with water. After equilibration at constant temperature (25.0 ± 0.5 °C), the suspension was filtered through a 0.22 μ m Millipore filter. The filtrate, after appropriate dilution with the mobile phase (described under HPLC analysis), was assayed for each paraben concentration, while the solid residue was examined by thermal analyses (DSC and TGA). The concentrations of both parabens in solution were then plotted against the total amount of the second paraben in the system. The compositions of both the solid and liquid phases at equilibrium for each preparation were thereby precisely determined.

X-ray Crystal Structure Determination—Large transparent prismatic crystals of propylparaben and butylparaben were grown from solution in methanol and cyclohexane, respectively, by slow evaporation of the solvent at ambient temperature and pressure. Crystal densities were measured at 20 °C by flotation in aqueous KI solution. Preliminary unit cell and space group data for each species were obtained from precession photographs taken with Cu K α -radiation ($\lambda = 1.5418$ Å). For the propylparaben crystal, the space group $P2_1/c$ was uniquely determined from the systematic absences, whereas for butylparaben, extinction conditions indicated the space groups Cc or $C2/c$. The latter, chosen on the basis of intensity statistics which indicated a centric distribution, was vindicated by successful structural solution and refinement.

Reflection intensity data were measured at 293(2) K on a Nonius Kappa CCD diffractometer using Mo K α radiation ($\lambda = 0.71069$ Å) and a crystal to detector distance of 35 mm. Both data collections involved $1.0^\circ \phi$ -rotations followed by $1.0^\circ \omega$ -rotations and exposure times per frame of 34 s (propylparaben) and 20 s (butylparaben), yielding 21849 and 11601 measured reflection intensities, respectively. Cell refinement and data reduction were performed with programs DENZO16 and maXus17. Both structures were solved by direct methods (program SHELXS8618) which revealed the non-hydrogen atoms of the two independent molecules in the asymmetric unit of the propylparaben crystal and the single molecule in that of the butylparaben crystal. The hydrogen atoms were located in difference electron-density maps; those attached to C were included in idealized positions in a riding model (C–H 0.93–0.97 Å) and the hydroxyl H atoms refined freely. All H atoms were treated isotropically and non-H atoms anisotropically. Full-matrix least-squares refinement on F^2 was performed with program SHELXL9319. The C atoms of the alkyl chain of the butylparaben molecule were found to be disordered, all four occupying two alternative sites each. Final refinement yielded site-occupancy factors of 0.61 and 0.39 for the two arrangements.

Powder X-ray Diffraction (PXRD)—PXRD traces were recorded on a Philips PW1050/25 goniometer with Cu K α -radiation ($\lambda = 1.5418$ Å) produced at 50 kV and 40 mA. The system was calibrated with a silicon standard which yielded peak positions of $28.45 \pm 0.01^\circ 2\theta$ before and after each scan. All samples were manually ground, sieved (through a 200 μ m screen), and packed successively in the same aluminum sample holder for reproducibility of conditions, taking care also to minimize preferred orientation effects. Full PXRD traces (scan speed $1.0^\circ 2\theta$ min⁻¹, step size $0.1^\circ 2\theta$, 2θ -range 8–32°) were recorded for pure ethylparaben (E), pure propylparaben (P), and the two solid phases obtained by recrystallization from water of mixtures of E and P of molar compositions 1:1 and 1:2, respectively.

PXRD traces in the narrow 2θ -range 23.0–26.5° were recorded for the same four samples. To optimize the resolution of these traces, each sample was scanned in three passes, accumulating the counts at a scan speed of $0.50^\circ 2\theta$ min⁻¹ with a step size of $0.02^\circ 2\theta$.

Indexing of reflections was achieved using program Lazy Pulverix²⁰ with single-crystal X-ray data (unit cell, space group, atomic coordinates, thermal parameters) for E and P as input.

Results and Discussion

Solubility—The solubility data from binary, ternary, and quaternary mixtures are collected in Table 1. It is evident that a decrease of P solubility in water (approximately 50%) can be detected only for mixtures containing also E (bold figures), as shown previously by McDonald et al.⁵ for the combination of the four parabens. Furthermore, a decrease (approximately 10%) of E solubility from all mixtures containing P is also seen.

Crystal Structures of Parabens—Table 2 summarizes the available single crystal X-ray data and selected physical properties of the four parabens under discussion. It should be noted that for compounds M, E, and P, the number of molecules per unit cell (Z) exceeds the site multiplicity of the general equivalent positions of the respective space groups, namely 4 for both Cc and $P2_1/c$. Thus, M contains three crystallographically independent molecules in the

Table 1—Solubilities of Parabens in Water (25.0 ± 0.5 °C, $M \times 10^2$) as Single Components (italics), Binaries, Ternaries (M + E + P, P + E + B, P + M + B, M + E + B), and quaternary (M + E + P + B) Mixtures^a

	M	E	P	B	M + E + P	P + E + B	P + M + B	M + E + B	M + E + P + B
M	1.610	1.681	1.681	1.680	1.640	—	1.630	1.580	1.680
E	0.598	<i>0.578</i>	0.514	0.563	0.521	0.496	—	0.555	0.527
P	0.220	0.111	<i>0.218</i>	0.209	0.111	0.109	0.211	—	0.110
B	0.113	0.109	0.104	<i>0.105</i>	—	0.110	0.111	0.108	0.110

^a Solubility values for E and P from mixtures containing both compounds are printed in boldface; $n \geq 4$; $cv \leq 3\%$.

Table 2—Selected Physical and Crystallographic Data of 4-Hydroxybenzoate Esters

	methyl (M) ¹³	ethyl (E) ¹⁴	propyl (P)	butyl (B)
system	monoclinic	monoclinic	monoclinic	monoclinic
space group	<i>Cc</i>	<i>P2₁/c</i>	<i>P2₁/c</i>	<i>C2/c</i>
<i>a</i> , Å	13.568(5)	11.765(4)	12.0435(2)	20.0870(7)
<i>b</i> , Å	16.959(7)	13.182(1)	13.8292(3)	8.2182(2)
<i>c</i> , Å	12.458(6)	11.579(4)	11.7847(3)	14.7136(5)
β , deg	130.10(3)	107.76(3)	108.63(1)	121.39(1)
<i>V</i> , Å ³	2192.9	1710.2	1860.0	2073.4
<i>d</i> , (calcd) g cm ⁻³	1.382	1.291	1.287	1.244
<i>d</i> , (measd) g cm ⁻³	1.361	1.25(1)	1.28(1)	1.23(1)
<i>Z</i>	12	8	8	8
<i>R</i> (on <i>F</i>)	0.054	0.056	0.090	0.062
obsd reflections	1098	2189	2922	1379
all reflections	—	—	3728	2121
<i>wR</i> ₂ (on <i>F</i> ²)	—	—	0.222	0.186
MW	152.15	166.18	180.2	194.23
formula	C ₈ H ₈ O ₃	C ₉ H ₁₀ O ₃	C ₁₀ H ₁₂ O ₃	C ₁₁ H ₁₄ O ₃
CAS reg. no ^a	99-76-3	120-47-8	94-13-3	94-26-8

^a Provided by author.

asymmetric unit while both E and P contain two. While the occurrence of more than one molecule in the asymmetric unit may suggest an incorrect choice of unit cell and/or space group, we have in these instances confirmed the data listed in Table 2 by preliminary X-ray photography of all three compounds and by successful structural refinements of not only compound P, but also M and E in recent structure redeterminations.²¹ Compound B, crystallizing in the space group *C2/c*, has *Z* equal to the number of general equivalent positions and therefore contains only one molecule in the asymmetric unit.

Full details of the crystal and molecular structures of P and B will be published elsewhere.²¹ For the purposes of the present study, however, the salient feature evident from a comparison of the space group and unit cell data is that compounds E and P are isostructural and different in crystal structure from either M or B. The term "isostructural" is used here in the sense defined by Kálmán and Párkányi²² to denote the fact that E and P crystallize in the same space group with very similar unit cell dimensions and with atomic coordinates which are in close correspondence for common atoms.

Details of the common crystal packing mode in the isostructural species E and P, as exemplified by compound P, are illustrated in Figure 1. This figure shows that the two crystallographically independent molecules (A, B) form separate, but structurally analogous, infinite chains by head-to-tail hydrogen bonding involving the OH group as donor and the carbonyl O atom as acceptor. Within a given chain, successive molecules are related by a 2-fold screw axis (*2*₁) parallel to *b*, array A being generated by the *2*₁ located at $x = 1/2, z = 1/4$ and array B by the *2*₁ at $x = 0, z = 1/4$. The symmetry-independent molecules A and B are nearly coplanar, and the resulting crystal structure, shown in projection in Figure 2, consequently has a distinctive layered nature. The layers lie midway between the (202)

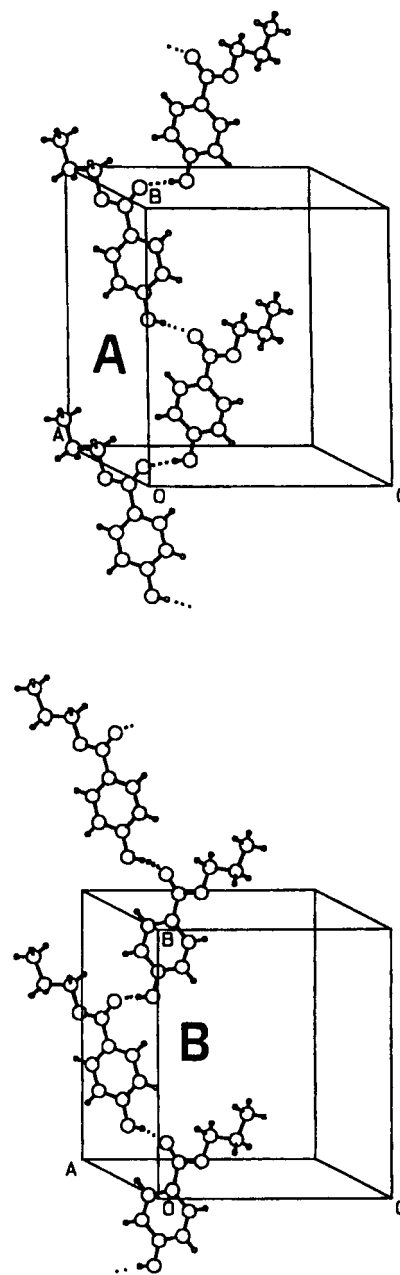


Figure 1—Head-to-tail hydrogen bonding arrays for the two crystallographically independent molecules A and B in propylparaben. Analogous arrays occur in the isostructural species ethylparaben.

crystal planes, thus accounting for the fact that the (202) reflection is predominant in the PXRD patterns of E and P.

A detailed exposition of the variations in molecular structures and packing modes for crystals of M, E, P, and B will be discussed elsewhere.²¹ Here, it is relevant to emphasize the isostructurality of E and P (both crystallizing in space group *P2₁/c*) and to contrast their common crystal packing arrangement with the different packing

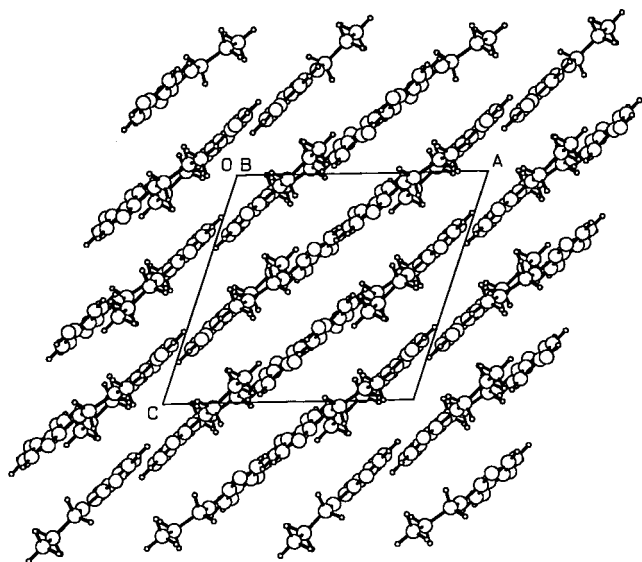


Figure 2—The [010] projection of the propylparaben crystal structure showing the characteristic molecular layers situated midway between the (202) planes.

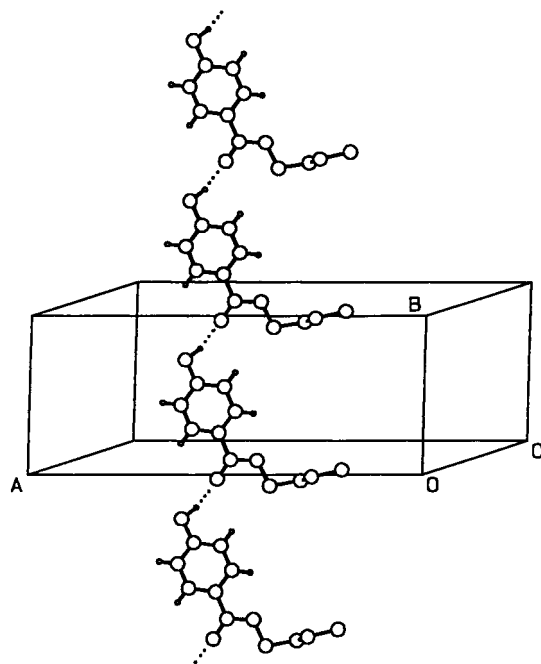


Figure 3—Head-to-tail hydrogen bonding array in the crystal of butylparaben. For clarity only the dominant conformer of the butyl chain is shown and the H atoms are omitted.

modes observed in M (Cc) and B ($C2/c$). The molecules in all four paraben crystals associate by head-to-tail (O—H \cdots O) hydrogen bonding, leading to infinite chains, as discussed above for E and P. However, successive molecules of the chains in E and P are generated by 2_1 -axes, whereas those in B are related by translation only, as shown in Figure 3. The resulting layered structure of B superficially resembles those of E and P, but the layers are distorted due to noncoplanarity of the butyl substituent and the aromatic ring as well as to the observed disorder of the butyl chain. The crystal packing mode in M is unique and complicated, owing to the presence of three symmetry-independent methyl paraben molecules. Alternate molecules in the hydrogen bonded chains have their aromatic ring planes nearly orthogonal to one another, giving rise to a complex packing arrangement¹³ devoid of the layers which are characteristic of the crystal structures of E, P, or B.

Table 3—Thermal Data^a of the Four Parabens

	methyl (M)	ethyl (E)	propyl (P)	butyl (B)
ΔH_f , J g ⁻¹	166.5 (4.9)	158.6 (5.0)	150.7 (4.7)	137.2 (4.2)
T_f , °C	126.0 (0.4)	115.8 (0.7)	96.1 (0.5)	68.6 (0.6)

^a $n \geq 4$; sd in parentheses.

Table 4—Observed and Calculated Eutectics for the Binary Systems

	M + E	M + P	M + B	E + P	E + B	P + B
X_{eut} , calcd ^a	0.46	0.35	0.78	0.40	0.24	0.33
T_{eut} , obsd, °C	86.5	76.5	57.0	—	59.0	55.0
T_{eut} , calcd, °C	88.5	77.8	59.8	76.0	58.3	54.6

^a Mole fraction of the first component of the binary system; values calculated by the intersection point of the liquidus curves obtained through the Schröder–Van Laar equation.

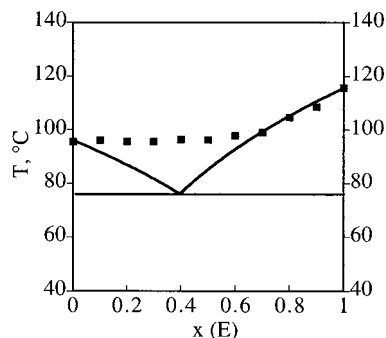


Figure 4—Phase diagram of the ethylparaben–propylparaben binary system. ■ = experimental points (onset temperatures from DSC measurements).

Cocrystallization, or solid solution formation, is a well-known consequence of isostructurality.²² For the four parabens involved, the increments in the volume of the asymmetric unit of the crystal through the series M \rightarrow E \rightarrow P \rightarrow B are 31.1, 18.7, and 26.7 Å³, the smallest of these being a consequence of the isostructurality of E and P. This fact indicates that the molecules of E and P, in these crystal packing arrangements, have a high degree of molecular complementarity; substitution of one molecule for the other during crystallization of physical mixtures should therefore be favored. This conjecture was explored by means of thermal methods of analysis and its validity subsequently confirmed by PXRD measurements.

Thermal Analytical Studies—Thermal data of the pure compounds and their binaries are collected in Tables 3 and 4. There was no evidence of any solvate formation (TGA measurements) for samples recrystallized from water or methanol.

While experimental data for binaries fit the calculated phase diagrams reasonably well for the combinations, M + E, M + P, M + B, E + B, and P + B, the plot of melting point against the mole fraction for the E + P system (Figure 4) shows a large plateau region up to a mole fraction for $x(E)$ value of about 0.6. No eutectic melting was observed at any composition, either in DSC runs or by HSM. It should be noticed that all melted samples readily recrystallized upon cooling; in all cases melting temperatures and heats measured during the second runs were not significantly different from those determined during the first runs.

These results suggest a solid solution behavior that is not far from ideal and that is probably substitutional, indicating a minimal disturbance of the crystal lattice when P molecules are progressively substituted by E, in the $x(E)$ range, 0 to 0.6. The smooth dependence of the melting point of E and P combinations on the mole fraction of either E or P, shown in Figure 4, has a barely perceptible minimum

at $x(E)$ near 0.4, which is close to the unrealized eutectic composition predicted by the Schröder–Van Laar equation in its simplified form (Table 4). This trend in melting point is paralleled by the enthalpies of fusion (ΔH^f , kJ mol^{-1} = 26.4 for pure E, minimum value of 20.5 at 0.436 $x(E)$, 27.5 for pure P) and consequently by the entropies of fusion (ΔS^f , $\text{J K}^{-1} \text{mol}^{-1}$ = 67.8 for pure E, minimum value of 55.1 at 0.436 $x(E)$, 74.1 for pure P). This behavior corresponds to a continuous series of solid solutions that show minor deviations from ideal behavior toward molecular segregation with weaker interactions between unlike molecules (E + P) than between like molecules (E + E or P + P). (Extreme deviations from ideality toward complete segregation would, of course, correspond to a eutectic system, often with limited miscibility in the solid state at compositions near the pure components).

A measure of the extent of lattice disorder created in the "host" crystal lattice by "guest" molecules in solid solution is provided by a dimensionless "disruption index" (d_i).²³ The d_i is evaluated as the negative slope of the plot of the molar entropy of fusion, ΔS^f , of the host (+ guest) against the ideal molar entropy of mixing, ΔS^m , of the host + guest at low mole fractions of the guest (additive or impurity molecules).²³ If the guest simply "dilutes" the host without causing any lattice disruption, both the solid solution and its liquid melt will behave as ideal solutions, so ΔS^f will not be changed by the presence of the guest and therefore the d_i will be zero. If the guest disrupts the crystal lattice of the host by forming lattice defects or imperfections, additional disorder will be created in the host crystal lattice but not in the liquid melt which is randomly disordered and probably behaves almost ideally, so ΔS^f will decrease significantly and the d_i will be appreciable. Thus, d_i measures the extent of disruption of the crystal lattice of the "host" by molecules of the "guest". For solid solution in which P is the host and E is the guest, the d_i is 0.6, suggesting very little lattice disruption. A similar, but less accurate, value is given by a solid solution in which E is the host and P is the guest. Small values of d_i less than 1.0 are also given by metallic systems, e.g., for Cd or In as the guest in InCd_3 as the host or for InCd_3 as the guest in Cd as the host. Evidently, the substitution of Cd atoms for In atoms and vice versa in these metallic systems gives little lattice disruption, presumably because the Cd and In atoms occupy similar volume;²³ they are also neighbors in the periodic table. The isostructurality of E and P (Table 2) readily explains the small value of d_i . On the other hand, the additional methylene group in the P molecule as compared with E explains the slight tendency toward molecular segregation deduced above from the plots of melting point, enthalpy of fusion, and entropy of fusion against mole fraction of E or P in the solid solution of E + P. By contrast, if the host and guest are different small organic molecules and therefore possess different crystal lattices, the d_i is appreciable and of the order 5 to 10.²³ If the host and guest are opposite enantiomers, or other closely related isomers, the d_i is significantly larger, of the order 20, because of the greater disorder (disruption) created by chiral discrimination in ordered structures.²⁴ If the host is a molecular crystal and the guest is a polymeric surfactant, d_i can be much larger, of the order 200.²⁵

Powder X-ray Diffraction Patterns—The PXRD traces for the pure phases E and P are shown superimposed in Figure 5. Each individual experimental pattern matches the computed pattern calculated from the corresponding single crystal X-ray data, confirming that the forms present are those listed in Table 2. The close similarity of the traces in Figure 5 confirms the isostructurality of E and P that is established above from the single crystal X-ray diffraction data. Furthermore, the peaks in the trace for P occur at

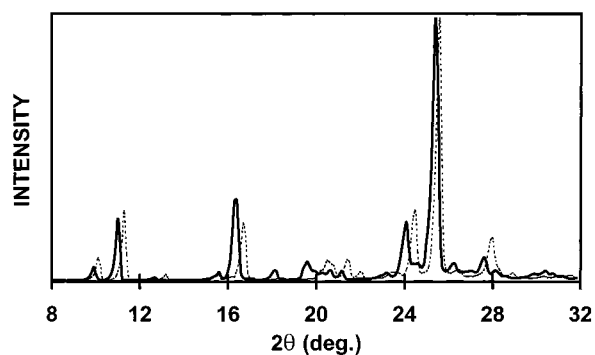


Figure 5—Powder X-ray diffraction patterns of pure propylparaben (solid trace) and pure ethylparaben (dotted trace).

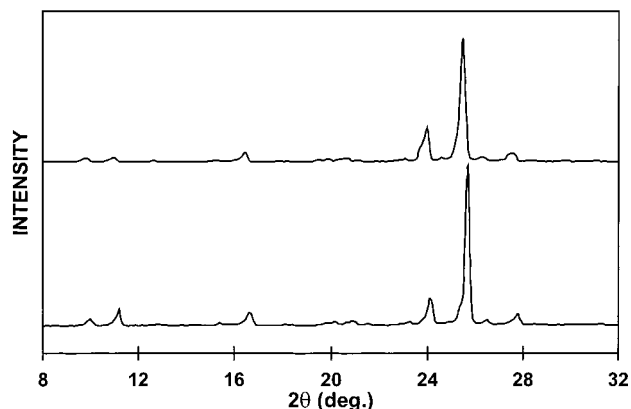


Figure 6—Powder X-ray diffraction patterns of two solid phases obtained by recrystallization of E/P mixtures with P:E molar ratios 2:1 (upper trace) and 1:1 (lower trace).

slightly lower 2θ -values than the corresponding peaks for E, in accordance with the larger unit cell parameters of P (Table 2).

To validate the partial conclusions suggested by thermal analyses and phase diagrams, the two samples obtained by recrystallization of P + E mixtures from water were subjected to a detailed study. While the original mixtures contained P:E molar ratios of 1:1 and 2:1, HPLC analyses yielded P:E molar ratios of 0.97:1 and 3:1 for the two recrystallized phases, respectively. Figure 6 shows the PXRD traces for these species. The close similarity of these traces to each other, and to those shown for the pure phases (Figure 5), leads to the conclusion that all four phases are isostructural, which strongly supports the notion that the phases obtained by recrystallization of physical mixtures are solid solutions of E and P.

For quantitative confirmation, the narrow 2θ -range 23.0–26.5° was selected, within which two prominent, representative diffraction peaks appeared for all four phases. From simulated patterns of E and P, these peaks were identified as the (310) and (202) reflections, with calculated 2θ -shifts, $\Delta(2\theta)$, of 0.52° and 0.26°, respectively, for the pure components E and P. Figure 7 shows the PXRD traces for E, P, and the two samples indicated as being solid solutions. It is evident from these traces that, as the percentage of P in the sample increases, there is a general shift of corresponding peaks to lower 2θ -values and hence to larger d spacings. This finding is consistent with the expected increase in unit cell volume, which should accompany progressive substitution of ethyl paraben molecules by propyl paraben molecules in the solid state. In support of this conclusion, which is based on the measurement of small angular differences, it is pertinent to note that, for the extreme members of the series of solid solutions, E and P, the experimental $\Delta(2\theta)$ values for the

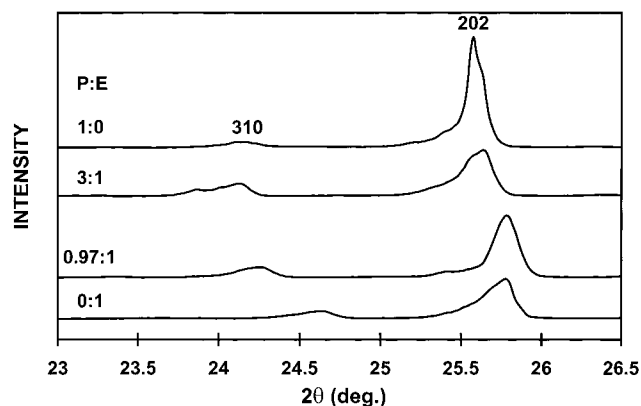


Figure 7—High-resolution powder X-ray diffraction patterns showing shifts of the (310) and (202) peaks as a function of P:E molar ratio in the solid phase.

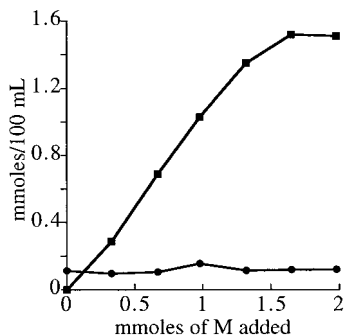


Figure 8—Phase-solubility diagram for the M + B system: ■ methylparaben, ● butylparaben ($n \geq 4$; $cv \leq 3\%$).

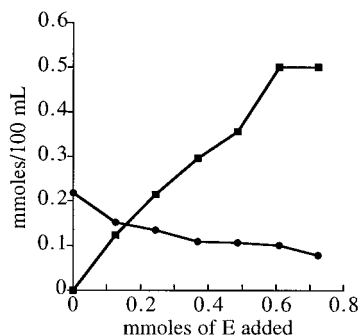


Figure 9—Phase-solubility diagram for the E + P system: ■ ethylparaben, ● propylparaben ($n \geq 4$; $cv \leq 3\%$).

(310) and (202) reflections are $\sim 0.5^\circ$ and $\sim 0.2^\circ$, in close agreement with the calculated values stated above. Because the unit cell involved is monoclinic, with the packing arrangement shown in Figures 1 and 2, progressive substitution of E molecules by P molecules is expected to lead to anisotropic unit cell expansion. From the data in Table 2, we note that the percentage increase in unit cell lengths on proceeding from E to P are 2.4, 4.9, and 1.8% for a, b, and c, respectively. In summary, the combined evidence from single-crystal X-ray diffraction and powder XRD studies confirms that E and P form substitutional solid solutions.

Phase-Solubility Investigations—The phase-solubility diagrams of the M + B and E + P systems are shown in Figures 8 and 9. When methylparaben is progressively added to a saturated solution of butylparaben, the saturation concentration of the latter (i.e., the solubility of B, circles in Figure 8) is not affected. The system becomes invariant (three phases and three components, at constant temperature and pressure) for both M and B, only when two solid phases are in equilibrium with a liquid phase

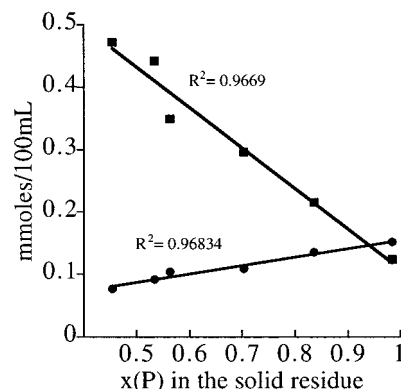


Figure 10—Relationship between composition of the solid phase at equilibrium and composition of the solution for each component: ■ ethylparaben, ● propylparaben. Data derived from phase-solubility analyses.

which is independently saturated by both compounds. Analogous patterns (not reported here) were found for other binaries.

For the E + P system, shown in Figure 9, the addition of increasing amounts of E to suspensions of P in water gives rise to a phase-solubility pattern that is different not only from the example reported above, involving no significant interaction between components, but also from the phase diagram for the formation of a solid stoichiometric complex.¹² In the E + P system, in fact, the concentration of the more abundant compound (P in this example) should remain constant until solid P is completely transformed into the solid solution P + E of lower solubility.

By plotting the data of Figure 9 as concentration of each paraben in the aqueous solution against the mole fraction of P in the solid residue, Figure 10 is obtained. It is evident that the solubilities of each paraben are affected by the presence of the second component. E can therefore be found in the solid-phase just after the first addition to a suspension of P in water, although its solubility is far below that of pure E.

Within the composition range explored and represented ($x(P)$ in the solid residue from 0.985 to 0.45), the solubilities of E and P are clearly linear functions of the solid composition at equilibrium.

Conclusions

The solubility behavior for propylparaben in the mixture of four components has been investigated in detail. As a necessary preliminary step, we simplified the quaternary system by examining all possible binary systems. The results clearly show that this peculiar behavior can be ascribed to the simultaneous presence of ethylparaben and propylparaben, as demonstrated by the individual solubility values for binary, ternary, and quaternary mixtures. Phase diagrams of all binaries show that, among all the systems investigated, P and E are the only pair that form almost ideal solid solutions.

Furthermore, phase-solubility analyses have shown that P and E at room temperature form solid solutions whose solubility is strictly related to the composition of the solid phase at equilibrium.

To obtain independent structural confirmation that solid solution formation explains the solubility behavior, the crystal structures of propylparaben and butylparaben have been solved, and the structural analogies between E and P have been demonstrated. PXRD of E, P, and their putative solid solutions each recrystallized from water show peaks whose 2θ -positions progressively shift as the composition proceeds from that of one pure compound to the other.

While not forgetting that crystallization is an irreversible, nonequilibrium process, the solid with the lowest chemical potential of E or P tends to crystallize out of the solution that contains both E and P. This solid solution contains a lower mole fraction of E and P than does pure E or P, respectively, because it has a lower chemical potential of E or P, respectively, and therefore has a lower solubility with respect to E or P. Therefore, if E is the solid in excess, E will tend to dissolve, whereas if P is the solid in excess, P will tend to dissolve, and the solid solution will crystallize out. The concentration of E or P in equilibrium with this solid solution (the measured apparent solubility) is less than that in equilibrium with pure E or P (the true solubility).

References and Notes

- Wade, A.; Weller, P. J., Eds. *Handbook of Pharmaceutical Excipients*, 2nd ed.; American Pharmaceutical Association: Washington, DC, 1994; pp 49–51, 191–193, 310–313, 411–414.
- Cohen, J.; Lach, J. L. Interaction of Pharmaceuticals with Schardinger Dextrins I. *J. Pharm. Sci.* **1963**, *52*, 132–136.
- Lach, J. L.; Cohen, J. Interaction of Pharmaceuticals with Schardinger Dextrins II. *J. Pharm. Sci.* **1963**, *52*, 137–142.
- Matsuda, H.; Ito, K.; Sato, Y.; Yoshizawa, D.; Tanaka, M.; Taki, A.; Sumiyoshi, H.; Utsuki, T.; Hirayama, F.; Uekama, K. Inclusion Complexation of p-Hydroxybenzoic Acid Esters with 2-Hydroxypropyl-beta-cyclodextrins. On Changes in Solubility and Antimicrobial Activity. *Chem. Pharm. Bull.* **1993**, *41*, (8), 1448–52.
- McDonald, C.; Palmer, L.; Boddy, M. The Solubility of Esters of 4-Hydroxybenzoic Acid, Determined Separately and Together, in Aqueous Solutions of 2-Hydroxypropyl- β -cyclodextrin. *Drug Dev. Ind. Pharm.* **1996**, *22*, 1025–1029.
- Grant, D. J. W.; Mehdizadeh, M.; Chow, A. H.-L.; Fairbrother, J. E. Nonlinear van't Hoff Solubility-temperature Plots and their Pharmaceutical Interpretation. *Int. J. Pharm.* **1984**, *18*, 25–38.
- Forster, S.; Buckton, G.; Beezer, A. E. The Importance of Chain Length on the Wettability and Solubility of Organic Homologs. *Int. J. Pharm.* **1991**, *72*, 29–34.
- Brittain, H. G.; Grant, D. J. W. Solubility of Pharmaceutical Solids. In *Physical Characterization of Pharmaceutical Solids*; Brittain, H. G. Ed.; Marcel Dekker: New York, 1995; pp 321–386.
- Khankari, R. K.; Grant, D. J. W. Pharmaceutical Hydrates. *Thermochim. Acta* **1995**, *248*, 61–79.
- Giron, D. Thermal Analysis and Calorimetric Methods in the Characterisation of Polymorphs and Solvates. *Thermochim. Acta* **1995**, *248*, 1–59.
- Giordano, F.; Bettinetti, G.; Cursano, R.; Rillosi, M.; Gazzaniga, A. A Physicochemical Approach to the Investigation of the Stability of Trimethoprim-Sulfamethoxazole (Co-Trimoxazole) Mixtures for Injectables. *J. Pharm. Sci.* **1995**, *84*, 1254–1258.

- Higuchi, T.; Connors, A. Phase-solubility Techniques. *Adv. Anal. Chem. Instr.* **1965**, *4*, 117–212.
- Lin, X., Studies on the crystal structure of p-substituted benzoates. I. The crystal structure of methyl p-hydroxybenzoate. *J. Struct. Chem.* **1983**, *2*, 213–217.
- Lin, X., Studies on the crystal structure of p-substituted benzoates. III. The crystal structure of ethyl p-hydroxybenzoate. *J. Struct. Chem.* **1986**, *5*, 281–285.
- Jacques, J.; Collet, A.; Wilen, S. H. *Enantiomers, Racemates, and Resolutions*; John Wiley & Sons: Interscience Publ.: New York, 1981; pp 46, 47.
- Otwinowski, Z.; Minor, W. Processing of X-ray diffraction data collected in oscillation mode. In *Methods in Enzymology*; Carter, C. W., Sweet, R. M., Eds.; Academic Press: New York, 1997; pp 307–326.
- Mackay, S.; Gilmore, C. J.; Edwards, C.; Tremayne, M.; Stewart, N.; Shankland, K. maXus: A Computer Program for the Solution and Refinement of Crystal Structures from Diffraction Data. University of Glasgow, Scotland, UK, Nonius BV, Delft, The Netherlands and MacScience Co. Ltd.: Yokohama, Japan, 1998.
- Sheldrick, G. M. SHELXS86. In *Crystallographic Computing 3*; Sheldrick G. M., Kruger, C., Goddard, R., Eds.; Oxford University Press: Oxford, UK, 1985; pp 175–178.
- Sheldrick, G. M. SHELXL93. Program for the Refinement of Crystal Structures, University of Göttingen, Germany, 1993.
- Yvon, K.; Jeitschko, W.; Parthe, E. J. LAZY PULVERIX, A Computer Program for Calculating X-ray and Neutron Diffraction Powder Patterns. *J. Appl. Crystallogr.* **1977**, *10*, 73–74.
- Caira, M. R.; Giordano, F.; Grant, D. J. W.; et al. Unpublished results.
- Kálmán, A.; Párkányi, L. Isostructurality of Organic Crystals: a Tool to Estimate the Complementarity of Homo- and Heteromolecular Associates. In *Advances in Molecular Structure Research*; Hargittai, M., Hargittai, I., Eds.; JAI Press: Greenwich, CT, 1997; Vol. 3, p 206.
- York, P.; Grant, D. J. W. A Disruption Index for Quantifying the Solid State Disorder Induced by Additives or Impurities. I. Definition and Evaluation from Heat of Fusion. *Int. J. Pharm.* **1985**, *25*, 57–72.
- Duddu, S. P.; Grant, D. J. W. The Use of Thermal Analysis in the Assessment of Crystal Disruption. *Thermochim. Acta* **1995**, *248*, 131–145.
- Al-Meshal, M.; York, P.; Grant, D. J. W. Disruptive Effects of Surfactant Molecules Incorporated into Phenylbutazone Crystals. *J. Pharm. Pharmacol.* **1985**, *37* (Suppl), 58.

Acknowledgments

F.G. and A.G. gratefully acknowledge financial support of Italian MURST (Ministero dell'Università e della Ricerca Scientifica e Tecnologica) and CNR (Consiglio Nazionale delle Ricerche). M.R.C. thanks the FRD (Pretoria) and the University of Cape Town for financial support. Part of this work was carried out in fulfilment of a Fulbright Scholarship of F.G. as Visiting Professor at the College of Pharmacy, University of Minnesota, Minneapolis. JS9900452